Journal of Applied Mechanics and Technical Physics, Vol. 49, No. 2, pp. 194–200, 2008

MODEL OF STEADY MOTION OF THE INTERFACE IN A LAYER OF A STRONGLY SUPERHEATED LIQUID

S. P. Aktershev and V. V. Ovchinnikov

UDC 536.423

Steady propagation of the boundary of a vapor cavity in a layer of a metastable liquid along the heater surface is considered. The temperature and velocity of interface propagation are determined from the equations of conservation of mass, momentum, and energy in the neighborhood of the stagnation point of the vapor cavity and the condition of stability of steady motion of the interface. It is shown that a solution of these equations exists only if the liquid is heated above a threshold value. The calculated velocity of interface motion and the threshold value of temperature are in reasonable agreement with available experimental data for various liquids within wide ranges of saturation pressures and temperatures of the superheated liquid.

Key words: *metastable liquid, interface, propagation velocity, superheating temperature.*

Introduction. The problem of growth of the vapor phase in a superheated liquid is important for understanding the fundamental features of the boiling process. In the general statement, this problem is extremely complicated, because the growth of the vapor phase depends on many interrelated factors: heat-transfer intensity, evaporation kinetics, liquid dynamics, etc. The experiments [1–4] revealed degeneration of the bubble boiling mode, when already the first emergence of the vapor phase led to formation of a stable vapor film, skipping the bubble boiling mode (third crisis of heat transfer). It was demonstrated [4] that there exists a lower boundary of superheating prior to incipience for the third crisis, and the values of heat fluxes in such a situation are lower than the values of the first critical flux. In this case, instability starts to develop in the contact zone between the vapor bubble surface and the heater, and conical vapor cavities propagating along the heater are formed (Fig. 1).

It was shown [5, 6] that the stagnation point of a conical vapor cavity (evaporation front) moves with a constant velocity. The velocity of the evaporation front substantially depends on liquid superheating and can reach tens of meters per second. The data on the evaporation front velocity for various organic liquids, water, and liquid nitrogen, were obtained in [5–11]. The experiments were performed at pressures both below and above the atmospheric value, with the use of a cylindrical heater and a plane heater under conditions of quasi-steady heating and a stepwise increase in power. It should be noted that the character of motion of the evaporation front is considerably different from the character of motion of the incipience wave, when the incipience zone consisting of isolated growing vapor bubbles propagates along the heated surface with an approximately constant velocity [6, 8]. In contrast to the incipience wave, the evaporation front is a moving interface. If the superheating is close to the threshold value, either the evaporation front or the incipience front can be observed; a transition from the incipience front to the evaporation front is also possible [8].

The evaporation front has some specific features and is of interest in studying the dynamics of a liquid with a free surface in the presence of a phase change. Though there are numerous experimental data, the mechanism of formation of the evaporation front has not been adequately studied, and the hydrodynamic features of such a flow are presented rather schematically. The numerical models developed in [12, 13] predict the velocity of propagation of the evaporation front. The model [12] also allows the threshold value of superheating to be calculated under the

---

Kutateladze Institute of Thermophysics, Siberian Division, Russian Academy of Sciences 630090; als@itp.nsc.ru. Translated from Prikladnaya Mekhanika i Tekhnicheskaya Fizika, Vol. 49, No. 2, pp. 47–55, March–April, 2008. Original article submitted May 4, 2007.

0021-8944/08/4902-0194

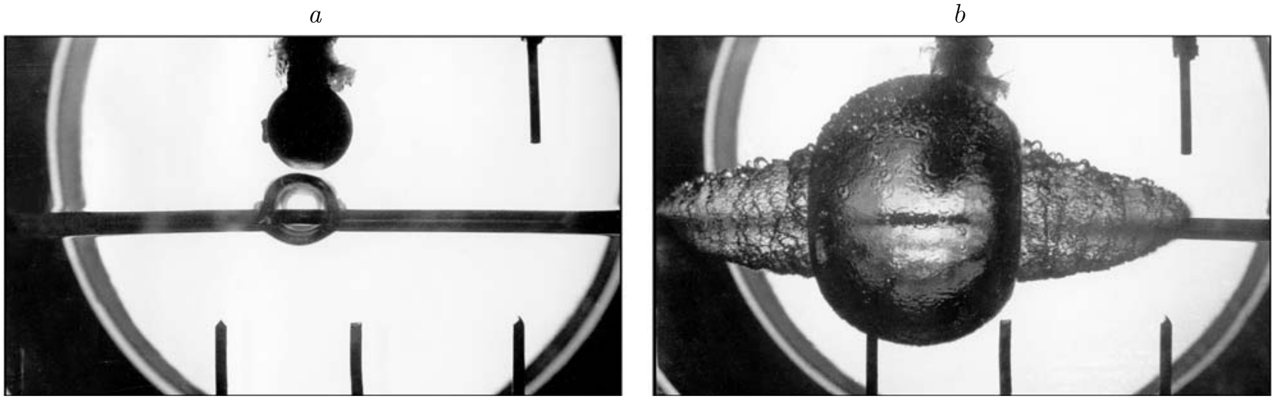

Fig. 1. Evaporation fronts formed during the growth of a vapor bubble in benzene on a cylindrical heater in 0.4 msec (a) and 4.8 msec (b) after incipience ($\Delta T = 86$ K and $T_s = 292$ K).

condition of the zero velocity of the evaporation front. It remains unclear, nevertheless, which dimensionless criteria exert a significant effect on the threshold value of superheating and interface velocity. The goal of the present study is to develop a simplified mathematical model of interface motion in a layer of a metastable liquid.

Mathematical Model. We consider a steady flow of a metastable liquid near the stagnation point of a vapor cavity in a reference system fitted to the evaporation front, which moves with a constant velocity V_f. The liquid near the heater surface has a temperature T_w and is superheated with respect to the saturation temperature T_s. Let us make the following simplifying assumptions: 1) the liquid is ideal, and the vapor is saturated; the vapor density is substantially lower than the liquid density; the liquid flow is two-dimensional; the vapor flow in the cavity is ignored; 2) evaporation is an equilibrium process, and the liquid and vapor temperatures on the interface coincide; the heat flux from the liquid to the interface is spent on evaporation only; 3) the velocity of the liquid on the interface is much smaller than the velocity of the evaporation front. Assumption No. 3 means that the velocity field of the liquid near the stagnation point in temperature calculations is the same as the field formed in the flow past an impermeable interface.

With allowance for the assumptions made, the equations of conservation of mass and momentum are written as the conditions [14] on the interface:

$$\rho_l u_l = \rho_v u_v = j; \tag{1}$$

$$p_l = p_v + j^2/\rho_v - \sigma/R. \tag{2}$$

Here u_l and u_v are the normal components of velocity, p_l and p_v are the pressures in the liquid and vapor phases, respectively, R is the radius of curvature of the interface, $j = (\lambda_l/L)\,\partial T_l/\partial r$ is the density of the mass flux, and L is the evaporation heat.

For the liquid, we write the Bernoulli equation along the streamline incoming from "infinity" to the stagnation point of the vapor cavity:

$$p_l = p_s + \rho_l V_f^2/2.$$

Here p_s is the pressure in the system. Substituting this relation into Eq. (2), we obtain

$$p_v - p_s = \rho_l V_f^2/2 - j^2/\rho_v + \sigma/R. \tag{3}$$

Equation (3) relates four unknowns: V_f, j, R, and the interface temperature T_v (the vapor pressure p_v and density ρ_v are functions of T_v). We can obtain another relation between these unknowns by considering heat transfer in the liquid in the vicinity of the stagnation point of the evaporation front.

We put the origin into the center of curvature of the frontal part of the vapor cavity and write the heat-transfer equation in the polar coordinate system

$$u_r \frac{\partial T}{\partial r} + \frac{u_\varphi \sin\varphi}{r} \frac{\partial T}{\partial \varphi} = a\Big[\frac{1}{r} \frac{\partial}{\partial r}\Big(r \frac{\partial T}{\partial r}\Big) + \frac{1}{r^2} \frac{\partial^2 T}{\partial \varphi^2}\Big] \tag{4}$$

with the boundary conditions

$$T\Big|_{r=R} = T_v, \qquad T\Big|_{r\to\infty} = T_w.$$

The velocity field of the liquid in the vicinity of the stagnation point is assumed to be identical to that formed in a potential flow around a cylinder of radius R:

$$u_r = (R^2/r^2 - 1)V_f \cos\varphi, \qquad u_\varphi = (R^2/r^2 + 1)V_f \sin\varphi.$$

Considering solutions near the stagnation point only, we can assume that $\varphi \ll 1$ and omit the second term in the left side of Eq. (4). Assuming also that

$$\frac{1}{r^2}\frac{\partial^2 T}{\partial\varphi^2} \ll \frac{\partial^2 T}{\partial r^2},$$

we reject the last term in the right side of Eq. (4).

Let us introduce the dimensionless variables $\eta = r/R$ and $\tilde{T} = (T - T_v)/(T_w - T_v)$. With these variables, Eq. (4) and the boundary conditions acquire the form

$$\mathrm{Pe}\Big(\frac{1}{\eta^2} - 1\Big)\eta\,\frac{\partial\tilde{T}}{\partial\eta} = \frac{\partial}{\partial\eta}\Big(\eta\,\frac{\partial\tilde{T}}{\partial\eta}\Big), \qquad \tilde{T}\Big|_{\eta=1} = 0, \quad \tilde{T}\Big|_{\eta\to\infty} = 1. \tag{5}$$

Here $\mathrm{Pe} = V_f R/a$ is the Peclet number. Integrating Eq. (5), we obtain

$$\frac{\partial\tilde{T}}{\partial\eta} = \frac{A}{\eta}\exp\Big(-\mathrm{Pe}\Big(\frac{1}{\eta} + \eta - 2\Big)\Big), \qquad A = \frac{\partial\tilde{T}}{\partial\eta}\Big|_{\eta=1}. \tag{6}$$

We introduce the variable $y = (\eta - 1)\sqrt{\mathrm{Pe}}$ and integrate Eq. (6). We obtain the following equation for the constant A with allowance for the boundary conditions:

$$\frac{A}{\sqrt{\mathrm{Pe}}}\int\limits_0^\infty \frac{\exp\left(-y^2/(1 + y/\sqrt{\mathrm{Pe}})\right)}{1 + y/\sqrt{\mathrm{Pe}}}\,dy = 1. \tag{7}$$

For $\sqrt{\mathrm{Pe}} \gg 1$, we can reject the terms $y/\sqrt{\mathrm{Pe}}$ in the integral of Eq. (7). Hence, we find $A = 2\sqrt{\mathrm{Pe}}/\sqrt{\pi}$ and the mass flux on the interface:

$$j = \frac{\lambda_l(T_w - T_v)}{RL}A = \frac{2}{\sqrt{\pi}}\frac{c_p(T_w - T_v)}{L}\rho_l\sqrt{\frac{V_f a}{R}}. \tag{8}$$

Substituting Eq. (8) into Eq. (3), we obtain an expression that relates three unknowns (V_f, R, and T_v):

$$p_v - p_s = \frac{\rho_l V_f^2}{2} - \frac{4}{\pi}\Big(\frac{c_p(T_w - T_v)}{L}\Big)^2\frac{\rho_l^2}{\rho_v}\frac{V_f a}{R} + \frac{\sigma}{R}. \tag{9}$$

We introduce three dimensionless criteria:

$$X = \frac{4}{\pi}\Big(\frac{c_p(T_w - T_v)}{L}\Big)^2\frac{\rho_l a}{\rho_v\sigma}\sqrt{2\rho_l(p_v - p_s)}, \qquad Y = \frac{\sigma}{R(p_v - p_s)}, \qquad Z = V_f\sqrt{\frac{\rho_l}{2(p_v - p_s)}}.$$

Here the criterion Y is the dimensionless curvature of the interface and the criterion X is the dimensionless temperature on the interface. Dividing both sides of Eq. (9) by $p_v - p_s$, we write it in dimensionless form as

$$Z^2 - ZXY + Y = 1. \tag{10}$$

If we consider X and Y as independent variables, then Eq. (10) determines the dimensionless velocity of the evaporation front $Z = Z(X, Y)$. To find three unknowns X, Y, and Z from Eq. (10), we have to use an additional relation based on some acceptable assumptions.

The photographs obtained in the experiments [5, 8] show that there are disturbances in the form of roughness or waves on the interface. We assume that the evaporation front velocity is insensitive to small fluctuations of interface curvature near the stagnation point of the cavity. This means that the value of the function $Z(X, Y)$ remains unchanged with small variations δY, i.e.,

$$\frac{\partial Z}{\partial Y} = 0. \tag{11}$$

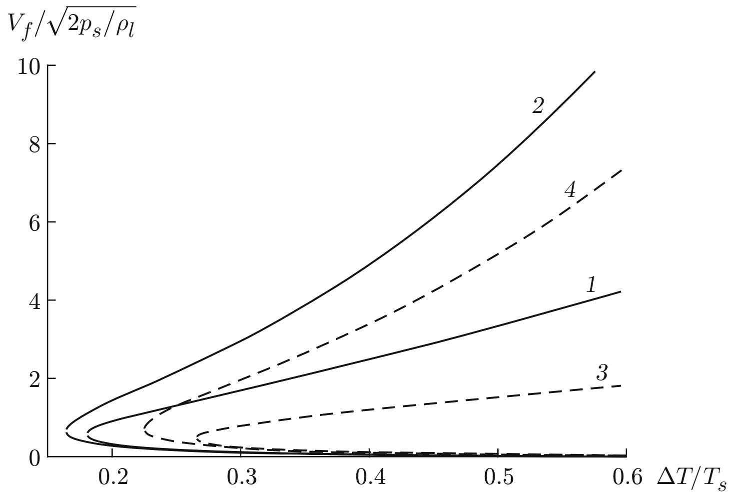

Fig. 2. Evaporation front velocity versus superheating for $\beta = 10$ (1 and 3) and $\beta = 20$ (2 and 4): curves 1 and 2 refer to $S = 0.01$ and curves 3 and 4 refer to 0.02.

From Eqs. (10) and (11), we obtain $X = 1$ and $Z = 1$, i.e.,

$$V_f = \sqrt{2(p_v - p_s)/\rho_l}; \tag{12}$$

$$\frac{4}{\pi}\Big(\frac{c_p(T_w - T_v)}{L}\Big)^2 \frac{\rho_l a}{\rho_v \sigma}\sqrt{2\rho_l(p_v - p_s)} = 1. \tag{13}$$

If we substitute the dependences $p_v(T_v)$ and $\rho_v(T_v)$ into Eq. (13), we can find the interface temperature T_v from this equation and then the velocity V_f from Eq. (12). Another alternative of the closing relation can also be considered. We assume that the dimensionless interface temperature X is a function of the independent variables Y, Z and that $\partial X/\partial Y = 0$ with small variations δY. This reasoning also implies, with allowance for Eq. (10), that $Z = 1$ and $X = 1$, i.e., we again obtain Eqs. (12) and (13). Note that the value of the criterion Y remains uncertain. Relations (12), (13) mean that the difference in pressure caused by capillary forces for all values of interface curvature is compensated by the reactive force of the evaporating liquid. The interface temperature and velocity turn out to be independent of curvature.

Calculation of Interface Velocity. Assuming the vapor to be an ideal gas with the equation of state $p_v = \rho_v R_g T_v$, we present the saturated vapor pressure as a function of temperature:

$$p_v = p_s \exp\Big(\frac{L}{R_v T_s}\Big(1 - \frac{T_s}{T_v}\Big)\Big). \tag{14}$$

We introduce the dimensionless interface temperature $\chi = (T_v - T_s)/\Delta T$, where $\Delta T = T_w - T_s$ is the value of superheating. Substituting Eq. (14) into Eq. (13), we write Eq. (13) in the form

$$F(\chi) = C. \tag{15}$$

Here

$$F(\chi) = (1-\chi)^2 \frac{1+\alpha\chi}{\tilde{p}(\chi)}\sqrt{\tilde{p}(\chi) - 1}, \quad C = \frac{S}{\alpha^2}, \quad S = \frac{\pi}{4}\Big(\frac{L}{c_p T_s}\Big)^2 \frac{\rho_{vs}}{\rho_l}\frac{\sigma}{a\sqrt{2\rho_l p_s}}, \quad \alpha = \frac{\Delta T}{T_s},$$

$\tilde{p}(\chi) = \exp(\beta\alpha\chi/(1+\alpha\chi))$ is the dimensionless pressure of saturated vapor, and $\beta = L/(R_g T)_s$. As the function $F(\chi)$ has zero values at the ends of the interval $0 < \chi < 1$, it reaches a maximum value $F_{\max}$ somewhere inside the interval. For $F_{\max} < C$, Eq. (15) has no solutions; for $F_{\max} > C$, Eq. (15) has two roots χ_1 and χ_2, which depend on the dimensionless parameters α, β, and S. As $C \sim 1/\Delta T^2$, Eq. (15) has solutions only if the superheating ΔT is greater than a certain threshold value ΔT_m. With increasing ΔT, the smaller root χ_1 decreases and the greater root χ_2 increases (for the threshold value of superheating, $\chi_1 = \chi_2$). Hence, Eq. (12) yields two branches of the dependence of the interface velocity on superheating: $V_1(\alpha)$ and $V_2(\alpha)$. With increasing ΔT, the function $V_2(\alpha)$ increases and $V_1(\alpha)$ decreases (for the threshold value of superheating, $V_1 = V_2 = V_m$).

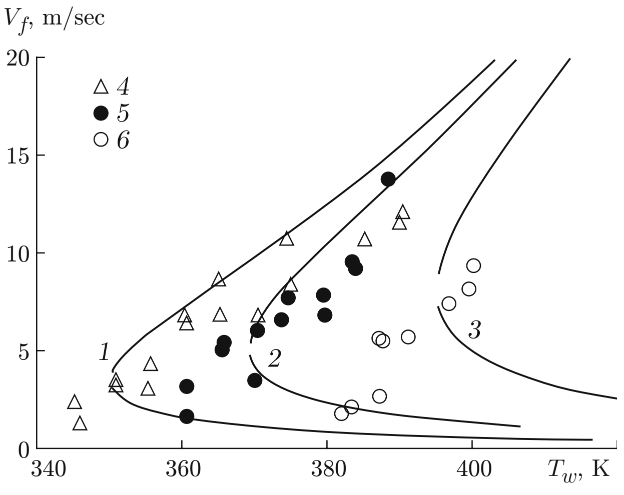

Fig. 3

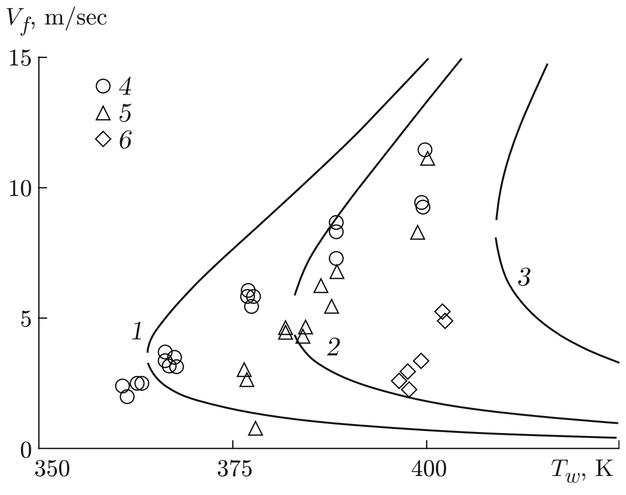

Fig. 4

Fig. 3. Dependence $V_f(T_w)$ for methanol for different values of T_s: curves 1–3 refer to the results calculated in the present work for $T_s = 290$ (1), 302 K (2), and 321 K (3); points 4–6 refer to the experimental data [7] for $T_s = 289.3$ (4), 302.1 (5), and 321.3 K (6).

Fig. 4. Dependence $V_f(T_w)$ for propanol for different values of T_s: curves 1–3 refer to the results calculated in the present work for $T_s = 307$ (1), 320 (2), and 340 K (3); points 4–6 refer to the experimental data [7] for $T_s = 307$ (4), 319.9 (5), and 339.1 K (6).

Equation (15) was solved numerically. Figure 2 shows the calculated dimensionless velocity of the evaporation front $V_f/\sqrt{2p_s/\rho_l}$ versus the dimensionless superheating $\alpha = \Delta T/T_s$ for different values of the parameters β and S. The threshold value α_m [a solution of Eq. (15) exists for $\alpha > \alpha_m$] depends on the value of the parameter S and increases with the latter. The value of the parameter β exerts a much smaller effect on the threshold value α_m. For $\beta \leqslant 10$ and $\alpha \gg \alpha_m$, the curve $V_2(\alpha)$ is close to a straight line. The slope of the curve $V_2(\alpha)$ is determined by the value of β, and the parameter S exerts a minor effect.

The results of the above-performed analysis of the solution of Eq. (15) are also valid if the dependences $p_v(T_v)$ and $\rho_v(T_v)$ are used for a real gas and if the temperature dependence of surface tension is taken into account. Indeed, relation (13) in dimensionless variables can be written in the form of Eq. (15), where

$$F(\chi) = \frac{(1-\chi)^2}{\tilde{\rho}_v \tilde{\sigma}} \sqrt{\tilde{p} - 1}, \qquad C = \frac{\pi}{4} \Big(\frac{L}{c_p \, \Delta T}\Big)^2 \frac{\rho_{vs}}{\rho_l} \, \frac{\sigma_s}{a\sqrt{2\rho_l p_s}},$$

$\tilde{\rho}_v(\chi) = \rho_v/\rho_{vs}$ and $\tilde{p}(\chi) = p_v/p_s$ are monotonically increasing functions; $\tilde{\sigma}(\chi) = \sigma/\sigma_s$ is a monotonically decreasing function. In further calculations, the thermophysical properties of particular substances [15] were approximated by smooth monotonic functions.

Calculation Results. The difference in the properties of vapor from the properties of an ideal gas does not change the character of the dependences $V_1(\alpha)$ and $V_2(\alpha)$ but only induces some quantitative differences. The calculated results were compared with the experimental data [5, 7] for various substances. Figures 3–5 show the calculated velocities of interface motion versus the liquid temperature and the experimental data for methanol, propanol, heptane [7], and water [5]. In the experiments, the parameter was $\Delta T/\Delta T_m \leqslant 1.5$, and the evaporation front velocity exceeded the calculated threshold values V_m by no more than a factor of 3. For different liquids at different saturation temperatures, the measured results agree with the calculated value of $V_2(\alpha)$ and differ substantially from the value of $V_1(\alpha)$. For each liquid, the threshold value of temperature T_m, above which propagation of the evaporation front is observed, increases with increasing saturation temperature. The calculated dependence $T_m(T_s)$ describes this phenomenon but yields slightly overpredicted values of T_m, as compared with the experimental data. In the experiments [7], the measurements were performed near the threshold values of superheating where it is difficult to distinguish between the evaporation front and the incipience front. With allowance for the scatter of the experimental data, the agreement with the calculated results is rather reasonable.

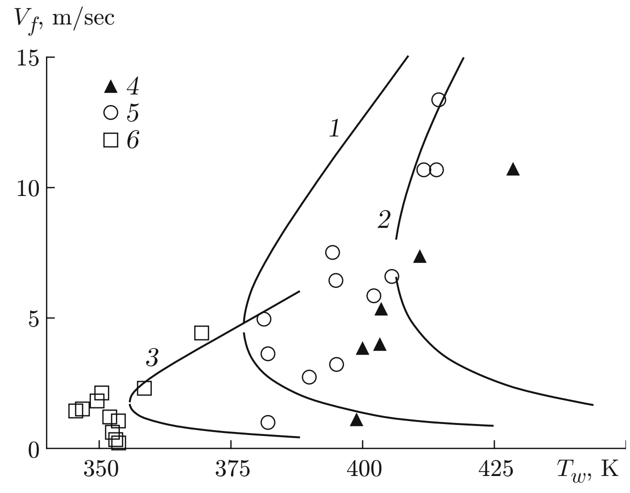

Fir. 5

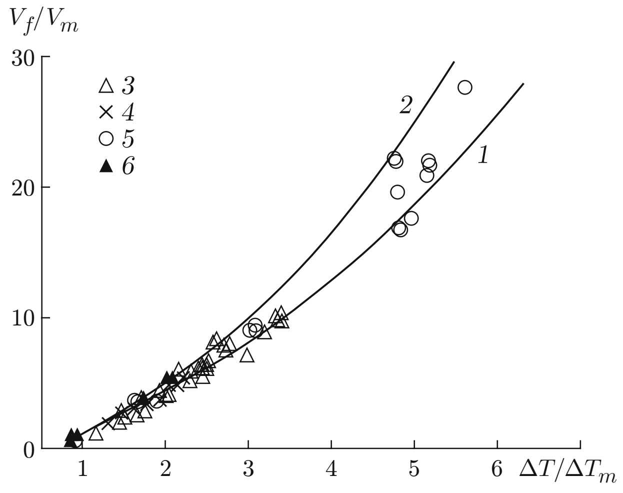

Fir. 6

Fig. 5. Dependence $V_f(T_w)$ for heptane (1, 2, 4, and 5) and water (3 and 6) for different values of T_s: curves 1–3 refer to the results calculated in the present work for $T_s = 325$ (1), 350 (2), and 300 (3); points 4–6 refer to the experimental data for $T_s = 349.8$ [7] (4), 325.2 [7] (5), and 294.2–304.6 K [5] (6).

Fig. 6. Evaporation front velocity versus superheating: curves refer to the calculated results for $\beta = 12$ and $S = 0.01$ (1) and $\beta = 12.7$ and $S = 0.02$ (2); points refer to the experimental data for benzene (3), acetone (4), toluene (5), and ethanol (6).

TABLE 1

Parameters of Experimental Regimes

Substance	d, m	T_s, K	ΔT, K	Reference
Acetone	$2.5 \cdot 10^{-3}$	297–321	94–146	[5]
Benzene	$2.5 \cdot 10^{-3}$	288–318	73–174	[5]
	$1.0 \cdot 10^{-4}$	288–289	187–213	[5]
Toluene	$1.0 \cdot 10^{-4}$	290–374	50–236	[5]
Ethanol	$2.5 \cdot 10^{-3}$	295–351	72–129	[5]
	$1.8 \cdot 10^{-2}$	302	51–81	[7]

Figure 6 shows the experimental data for acetone, benzene, toluene [5], and ethanol [5, 7] for a rather wide range of superheating. The results are plotted in dimensionless variables; the temperature and velocity scales are the calculated threshold values ΔT_m and V_m. In these experiments, the front velocity exceeded V_m by a factor of several tens. The experimental regimes are summarized in Table 1 (d is the heater diameter). It follows from Fig. 6 that the experimental points for these substances are grouped near one line. This fact has a simple explanation. All four substances examined have similar thermophysical properties, and the changes in saturation temperature in all experiments was rather small. The value of the parameter $\beta = L/(R_g T)_s$ responsible for the slope of the curve was approximately the same for these substances. Figure 6 also shows two curves calculated for $\beta = 12$, $S = 0.01$ and $\beta = 12.7$, $S = 0.02$. In the interval $\Delta T/\Delta T_m \leqslant 3$, these curves are close to each other, and most experimental points stay between these curves.

In calculating the liquid temperature in the vicinity of the stagnation point, we assumed that $\text{Pe} \gg 1$ and that the interface is impermeable. Using Eq. (8), we can estimate the ratio of the liquid velocities on the interface and at "infinity" as

$$\frac{u_l}{V_f} = \frac{j}{\rho_l V_f} \approx \frac{c_p\,\Delta T}{L}\,\frac{1}{\sqrt{\text{Pe}}}.$$

In the experiments [5, 7], the inequality $c_p \Delta T/L \leqslant 0.5$ was satisfied for superheating. If we assume that the radius of curvature at the stagnation point of the vapor cavity is greater than 10^{-6} m, we obtain $\mathrm{Pe} \geqslant 100$ for the values $V_f \approx 10$ m/sec reached in the experiments, and $u_l/V_f \leqslant 0.05$. Thus, the assumptions made are acceptable for the experimental conditions. It should be noted that the experimental data [5, 7] were obtained for heaters of different diameters and different wall materials during both steady heating and a stepwise increase in power. The thickness of the superheated layer of the liquid was also substantially different for different heaters. Nevertheless, the experimental data for different substances in wide ranges of superheating and interface velocity are in reasonable agreement with the calculated results, which proves that this model is adequate.

Conclusions. A model of steady propagation of the interface in a metastable liquid is developed; the model implies that the interface propagation velocity is independent of surface curvature at the stagnation point of the vapor cavity. The interface temperature and velocity are determined by the properties of the superheated liquid and saturated vapor only. It is shown that the solution exists only if the temperature of the metastable liquid is higher than a certain threshold value. The dependence $V_2(\alpha)$ of interface velocity on superheating also has a threshold character.

This work was supported by the Russian Foundation for Basic Research (Grant No. 06-08-01501).

REFERENCES

1. S. J. D. Van Stralen, “Heat transfer to boiling binary liquid mixtures at atmospheric and sub-atmospheric pressures,” *Chem. Eng. Sci.*, **5**, 290–296 (1956).
2. J. H. Lienhard and V. E. Schrock, “The effect of pressure, geometry and the equation of state upon the peak and minimum boiling heat flux,” *Trans. ASME, Ser. C, Heat Transfer*, **85**, No. 3, 261–272 (1963).
3. N. N. Mamontova, “Boiling of certain liquids at reduced pressures,” *J. Appl. Mech. Tech. Phys.*, **7**, No. 3, 94–98 (1966).
4. B. P. Avksentyuk, G. I. Bobrovich, S. S. Kutateladze, and V. N. Moskvicheva, “The degeneration of nucleate boiling conditions under conditions of free convection,” *J. Appl. Mech. Tech. Phys.*, **13**, No. 1, 59–62 (1972).
5. B. P. Avksentyuk, V. V. Ovchinnikov, and V. Ya. Plotnikov, “Self-sustained incipience front and the third crisis of boiling,” in: Unsteady Processes in Two-Phase Flows (collected scientific papers) [in Russian], Inst. Thermophys., Sib. Div., Acad. of Sci. of the USSR, Novosibirsk (1989), pp. 52–68.
6. S. A. Zhukov and V. V. Barelko, “Dynamic and structural aspects of the processes of single-phase convective heat transfer, metastable regime decay and bubble boiling formation,” *Int. J. Heat Mass Transfer*, **35**, No. 4, 759–775 (1992).
7. J. Fauser and J. Mitrovic, “Some features of boiling fronts on heated surfaces,” in: *Heat Transfer*, Proc. of the 11th Int. Heat Transfer Conf. (Kyongju, Korea, August 23–28, 1998), Vol. 2, Taylor & Francis Inc., Philadelphia (1998), pp. 377–382.
8. B. P. Avksentyuk and V. V. Ovchinnikov, “Evaporation dynamics at superatmospheric pressure,” *J. Appl. Mech. Tech. Phys.*, **37**, No. 6, 850–856 (1996).
9. K. Okuyama and Y. Iida, “Transient boiling heat transfer characteristics of nitrogen (bubble behavior and heat transfer rate at stepwise heat generation),” *Int. J. Heat Mass Transfer*, **33**, No. 10, 2065–2071 (1990).
10. K. Okuyama, Y. Kozawa, A. Inoue, et al., “Transient boiling heat transfer characteristics of R113 at large stepwise heat generation,” *Int. J. Heat Mass Transfer*, **31**, No. 10, 2161–2174 (1988).
11. A. N. Pavlenko and V. Yu. Chekhovich, “Heat transfer crisis at transient heat release,” *Russ. J. Eng. Thermophys.*, **1**, No. 1, 73–92 (1991).
12. B. P. Avksentyuk, “Nonequilibrium model of an evaporation front,” *Russ. J. Eng. Thermophys.*, **5**, No. 1, 1–9 (1995).
13. A. N. Pavlenko and V. V. Lel’, “Approximate numerical model of a self-sustained evaporation front,” *Teplofiz. Aéromekh.*, **6**, No. 1, 111–124 (1999).
14. R. I. Nigmatulin, *Dynamics of Multiphase Media*, Part 1, Hemisphere Publ., New York (1991).
15. *Heat Exchanger Design Handbook*, Vol. 5: *Physical Properties*, Hemisphere Publ. Co., New York (1983).